CFD-DEM Simulation of Minimum Fluidisation Velocity in Two Phase Medium

H. A. Khawaja, PhD Student,
Department of Engineering, University of Cambridge, UK
hak23@cam.ac.uk

ABSTRACT

In this work, CFD-DEM (computational fluid dynamics – discrete element method) has been used to model the 2 phase flow composed of solid particle and gas in the fluidised bed. This technique uses the Eulerian and the Langrangian methods to solve fluid and particles respectively. Each particle is treated as a discrete entity whose motion is governed by Newton's laws of motion. The particle-particle and particle-wall interaction is modelled using the classical contact mechanics. The particles motion is coupled with the volume averaged equations of the fluid dynamics using drag law.

In fluidised bed, particles start experiencing drag once the fluid is passing through. The solid particles response to it once drag experienced is just equal to the weight of the particles. At this moment pressure drop across the bed is just equal to the weight of particles divide by the cross-section area. This is the first regime of fluidization, also referred as 'the regime of minimum fluidization'.

In this study, phenomenon of minimum fluidization is studied using CFD-DEM simulation with 4 different sizes of particles 0.15 mm, 0.3 mm, 0.6 mm, and 1.2 mm diameters. The results are presented in the form of pressure drop across the bed with the fluid superficial velocity. The achieved results are found in good agreement with the experimental and theoretical data available in literature.

1. INTRODUCTION

A fluidised bed consists of a fluid-solid mixture that exhibits fluid-like properties, e.g. objects with a higher density than the bed will sink, whereas objects with a lower density than the bed will float.

Fluidization occurs when a fluid (liquid or gas) is pushed upwards through a bed of granular material. At a low superficial gas velocity, the drag on each particle is also low, and thus the bed remains in a fixed state (i.e. a packed bed) as shown in Figure 1 (a). At a critical value of the superficial gas velocity, the upward drag force will exactly equal the downward gravitational force on the particles, causing the particles to become suspended within the fluid. At this critical velocity, usually denoted by U_{MF}, the bed is said to be fluidised and will exhibit fluid like behaviour, shown in Figure 1 (b). At this gas velocity, the pressure drop across the bed balances the net weight of the particles divided by the bed area, $\left(\Delta P = \frac{W}{A}\right)$.

Once a bed of particles is fluidised, its behaviour depends on the superficial gas velocity, particle density, and fluid properties and generally falls into one of 6 regimes. Increasing the superficial velocity beyond U_{MF} causes the bed to expand uniformly as shown in Figure 1 (c), giving rise to 'smooth fluidization'. The pressure drop across the bed remains equal to the

weight of particles per unit area. When the superficial velocity is increased beyond U_{MB} (minimum bubbling velocity), bubbles form as shown in Figure 1 (d). For large particles, fluidised by gas, U_{MB} is almost equal to U_{MF}, and the bed will begin to bubble as soon as the fluid velocity exceeds U_{MF}. With further increase in the fluid velocity, the frequency of bubble generation increases and bubbles start to coalesce. If the bubble diameter becomes comparable to the tube diameter, slugging is observed. Both round nosed slugs and flat nosed slugs can form as shown in Figure 1 (e) and (f). With a further increase in the fluid velocity, the upper bed boundary becomes less distinct and bubbles begin to break up. This is known as 'turbulent fluidization' as shown in Figure 1 (g). At even higher fluid velocities 'pneumatic transport' of the particles starts as shown in Figure 1 (h) [Kunii & Levenspiel (1991), Lee & Lee (2005)].

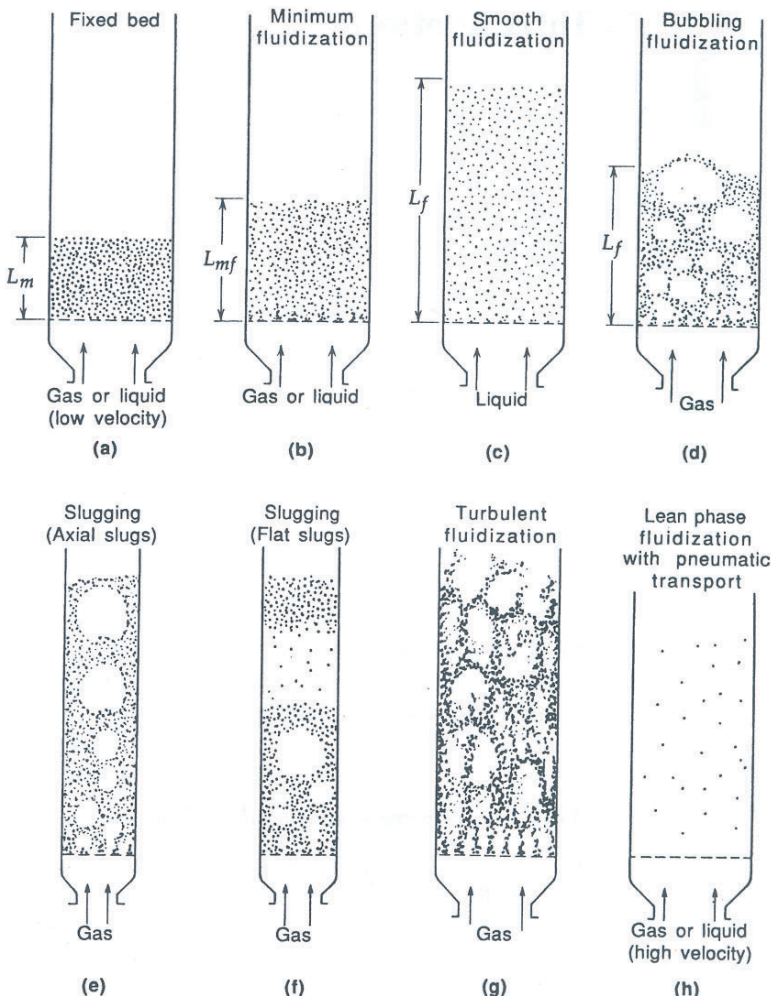

Figure 1 Regimes of fluidization: (a) Fixed Bed, (b) Minimum Fluidization, (c) Smooth Fluidization, (d) Bubbling Bed, (e) Axial Slugging Bed, (f) Flat Slugging Bed, (g) Turbulent Fluidization, (h) Pneumatic Transport [Reproduced from Kunii & Levenspiel (1991)].

The behaviour of the fluidised bed is strongly dependent on the types of particles used. Geldart proposed classifying particles into one of four groups. [Kunni & Levenspiel (1991)].

Geldart Group A: For this group, the particle size is between 20 and 100 μm, and the particle density is typically 1400kg/m^3. Prior to the initiation of a bubbling bed phase, beds from these particles will expand by a factor of 2 to 3 at incipient fluidization, i.e. just at the beginning of fluidization. Thus, particles are generally used in catalytic reactors.

Geldart Group B: The particle size lies between 40 and 500 μm and the particle density between 1400 and 4500 kg/m^3. Bubbles typically form directly at incipient fluidization, $U_{MF} \approx U_{MB}$.

Geldart Group C: This group contains extremely fine and subsequently the most cohesive particles. With a size of 20 to 30 μm, these particles are difficult to fluidise and may require additional agitation.

Geldart Group D: The particles in this group have diameters above 600 μm and typically have high particle densities. Fluidization of this group requires very high fluid energies and is typically associated with high levels of abrasion.

2. MINIMUM FLUIDIZATION VELOCITY

The minimum fluidization velocity (U_{MF}) is the minimum superficial velocity of fluid needed to fluidise a bed. At U_{MF} the net weight of the bed (the weight of the solids minus the buoyant force due to the displaced fluid) per unit area of bed is exactly balanced by the pressure drop over the bed, i.e.

$$\frac{\Delta P}{L_m} = \left(1-\varepsilon_{mf}\right)\left(\rho_s - \rho_f\right)g \qquad (1)$$

Where ΔP is the pressure drop of the fluid across the bed, L_m is the length of bed, ε_{mf} is the voidage in bed, ρ_s is the density of solid particles, ρ_f is the density of fluid and g is the gravitational constant. If we consider a total mass balance on the solids, assuming that no solids are entrained and carried out of the bed, then the total mass of solids is

$$M_s = \rho_s\left(1-\varepsilon_{mf}\right)AL_m \qquad (2)$$

where A is the cross-section area of bed.

For liquids and for gases, as long as the pressure drop is small, the fluid phase density is constant. Hence, the right hand side of Eqn. (1) is constant and thus the pressure drop in a fluidised bed is constant independent of the fluidizing velocity. Also it is observed through experimentation that if the bed is densely packed initially the pressure drop overshoots the fluidization pressure until the particles separate and fluidise. This is further illustrated in Figure 2. For a packed bed, Ergun et al. (1952) gives the frictional pressure drop, per unit length as

$$\frac{\Delta P}{L_m}\left(\frac{150\left(1-\varepsilon_{mf}\right)^2}{\varepsilon_{mf}^3}\right)\frac{\mu U}{\left(\phi_s d_p\right)^2} + 1.75\left(\frac{1-\varepsilon_{mf}}{\varepsilon_{mf}^3}\right)\left(\frac{\rho_f U^2}{\phi_s d_p}\right) \qquad (3)$$

Where μ is the viscosity of the fluid, ϕ_z is the sphericity of particles, ρ_f is the density of fluid, and U is the superficial velocity of the fluid.

At the onset of fluidization the bed is still packed, and the pressure drop is given by the Ergun's Equation. Substituting Eqn. (3) into Eqn. (1), gives

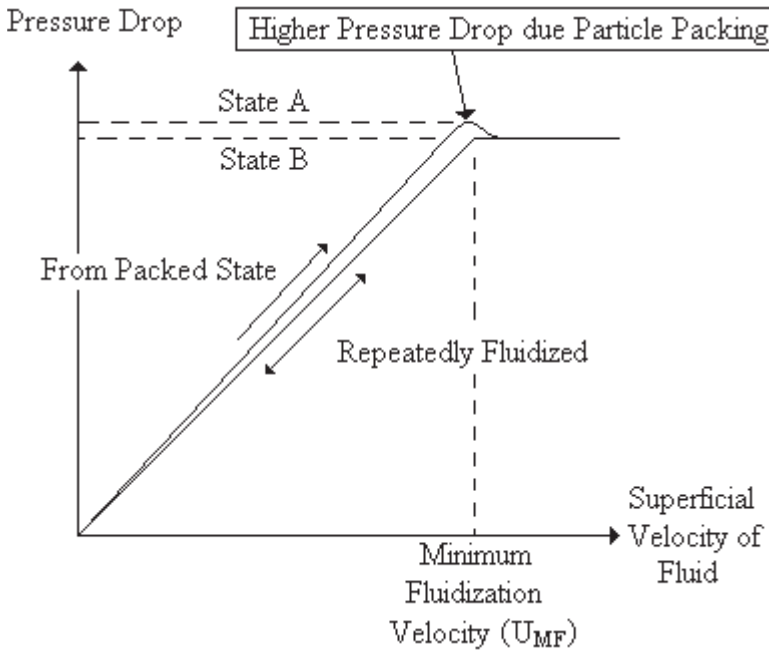

Figure 2 Generic pressure drop versus superficial velocity in packed and un-packed state.

$$\frac{1.75}{\varepsilon_{mf}^3\phi_s}\left(\frac{d_p U_{MF}\rho_f}{\mu}\right)^2+\frac{150\left(1-\varepsilon_{mf}\right)}{\varepsilon_{mf}^3\phi_s^2}\left(\frac{d_p U_{MF}\rho_f}{\mu}\right)=\frac{d_p^3\rho_f\left(\rho_s-\rho_f\right)g}{\mu^2} \quad (4)$$

If ε_{mf} is known at minimum fluidization, e.g. determined experimentally, Eqn. (4) can be used to determine minimum fluidization velocity (U_{MF}).

By introducing Reynolds number, $Re_{p,mf}\frac{d_p U_{mf}\rho_f}{\mu}\cdot$ and Archimedes number, $Ar=\frac{d_p^s\rho_f(\rho_s-\rho_f)g}{\mu^2}$, a non-dimensional form of Eqn 1.4 is obtained, i.e.

$$K_1 Re_{p,mf}^2+K_2 Re_{p,mf}=Ar \quad (5)$$

Where K_1 and K_2 are non-dimensional coefficients which are the functions of the voidage and sphericity of particles, and are given by,

$$K_1=\frac{1.75}{\varepsilon_{mf}^3\phi_s} \quad (6)$$

$$K_2=\frac{150\left(1-\varepsilon_{mf}\right)}{\varepsilon_{mf}^3\phi_s^2} \quad (7)$$

Table 1: Values of coefficients of modified Ergun's equation (Eqn. (5)).

Particle Size	$\frac{K_2}{2K_1}$	$\frac{1}{K_1}$
Fine (Wen and Yu (1966))	33.7	0.0408
Coarse (Chitester et al. (1984))	28.7	0.0494

Wen and Yu (1966) noted that these non-dimensional coefficients stay nearly constant over a wide range of particles and for $0.001 < Re_{p,mf} < 4000$; thus giving a prediction of U_{MF} with a 34% standard deviation. Values of K_1 and K_2 according to particles sizes are given in Table 1.

3. CFD-DEM MODEL

There are various models for simulating solid-gas phases simultaneously as discussed in Hoef et al. (2008). Here, the 2-phase flow in a gas-fluidised bed is simulated using an Eulerian (unresolved) model for the fluid modeling and Lagrangian particle tracking for the granular solids. The volume average Navier-Stokes equation, continuity equation and energy equation were solved [Anderson and Jackson (1967)]. The equations were discretised using central difference method and the time dependent terms are discretised using the methods of lines [Anderson, (1995)]. The 3rd Order Adams-Bashford [Hairer et al. (1993)] explicit scheme has been used to advance the conservative variables. The fluid was assumed to be compressible and the pressure field was computed using the ideal gas relationship. For stability, grid size has to be sized according to Courant Friedrichs Lewy (CFL) [Courant et al. (1967)] number.

The particles were modeled as 'soft' solid spheres meaning that the material can deform on contact with other spheres. Force relating displacement and velocity is given by Cundall and Strack (1979) based on classical contact mechanics relation given by Hertz et al. (1882) and Mindlin and Deresiewicz's (1953). This scheme is same as used by Tsuji et al. (1992). Interaction forces between particles and fluid was captured using drag law defined by Beestra et al. (2007). The normal and tangential forces are thus summed. The motion of particles was then found by integrating Newton's second law.

4. CFD-DEM FORTRAN CODE

The CFD-DEM code is written in FORTRAN and is divided into 2 main parts. The DEM code computes particle interaction using the Lagrangian method of solution. The CFD code computes fluid field by solving the volume averaged fluid equations. The code is written in the form of a library of subroutines, which can be called in various ways to customize the simulation, e.g. only particles in bed for e.g. kiln (only particles), incompressible fluid in bed of particles, compressible fluid in bed of particles.

The flow chart of the CFD-DEM code is presented in Figure 3. Code is initialized with particles positions, location of walls and the material specifications. First loop runs for boxing the particles and saving the number of contacts. Any misplaced (out of domain or overlapping) particle prompts an error. Also it recommended that particles are in no contact position, otherwise severe overlap can generate significant force to position the particle outside the domain. Computations start with calculation of particle acceleration, velocity and displacement. This process is looped for all particles involved. It should be noted here that resultant force (resultant of contact forces, gravity force and fluid drag; if fluid is involved) is used for the computations of these parameters. During initialization contact forces are unknown (zero) so it is required that particles must be initialized under no contact state.

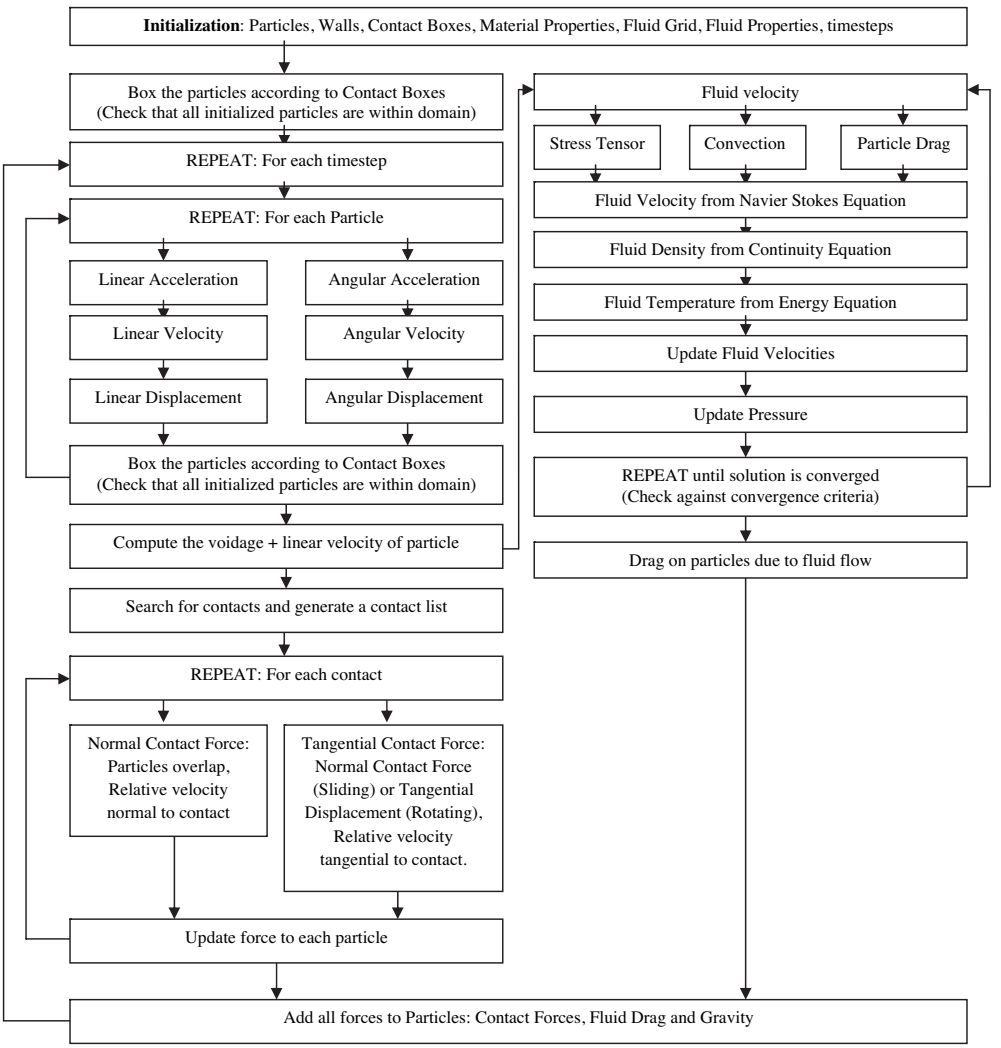

Figure 3 Flow chart of incompressible CFD-DEM code

Computations of contacts start right after positioning of particles. For the computations of tangential forces, sliding criteria is checked. This process is looped until all contacts are solved. Forces due to contacts are fed back to each particle responsible for it. It should be noted here that particle could be in position of having more than one contact. So, each particle can be fed with number of forces based on it contacts made with its surroundings (particles or wall). Particles are re-boxed and number of contacts are noted and saved. Then code is stepped forward in time.

If simulation is for 2 phase flow, voidage is computed after positioning the particles. Then, fluid field is computed. Final output of fluid code is the drag force over the particle added back to other forces acting i.e. contact forces, gravity, etc (used in computations of acceleration, velocity and displacement of particles).

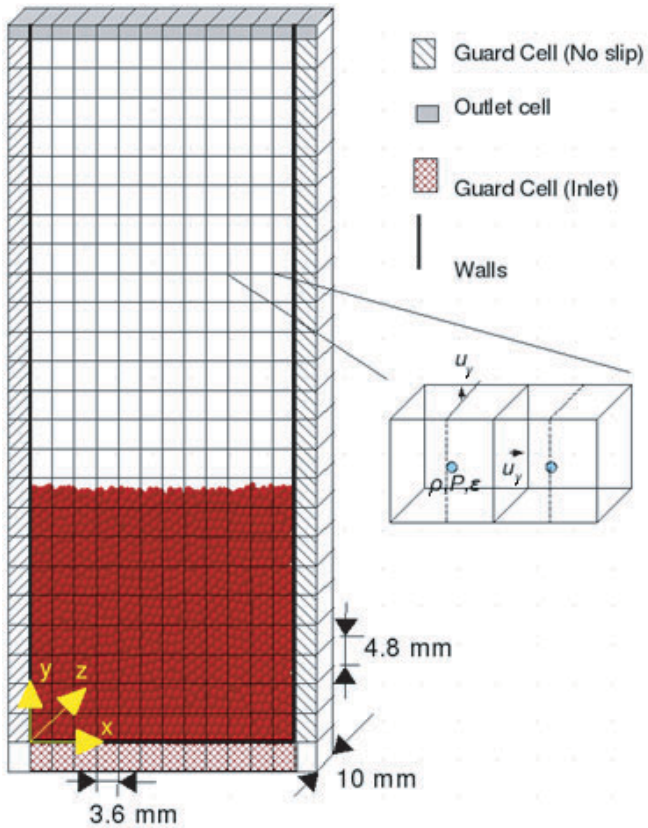

Figure 4 CFD-DEM domain of fluidised bed simulation.

This complete code is run in loops until the desired number of time steps are completed. For debugging and tracing the unusual crash of program, text outputs have been specified in almost every subroutine involved.

5. SIMULATION SETUP

The simulated bed setup is shown below in Figure 4. The particles were allowed to move in three dimensions, but due to the narrow domain, the fluid flow was modelled as two dimensional. This was achieved by using a single fluid cell in the 3rd dimension. Fluid was supplied uniformly through the base with a specified mass flux (achieved by specifying the rate of change of mass flux with time). No slip for the fluid was assumed on the walls. At the exit, an outflow condition was used; for the incompressible simulation, zero gradient in each component of the velocities were assumed, and for the compressible simulation a characteristic boundary condition was applied at the outlet. Simulations were performed with nominal particle diameters of 1.2 mm, 0.6 mm, 0.3 mm and 0.15 mm, and the domain scaled to give geometric similarity, meaning that the number of particles (and computational load) remained the same. This range of particle sizes covers two different Geldart groups; D and B.

Simulation parameters values are specified in Table 2.

Table 2 : Simulation parameters with particle sizes.

Parameters	*1.2mm Particles (Geldart D)*	*0.6mm Particles (Geldart D)*	*0.3mm Particles (Geldart B)*	*0.15mm Particles (Geldart B)*
Bed Width (x-direction)	0.0432m	0.0216m	0.0108m	0.0054m
Bed Height (y-direction)	0.1176m	0.0588m	0.0294m	0.0147m
Bed Thickness (z-direction)	0.01m	0.005m	0.0025m	0.00125m
Total Number of Fluid Cells	14 ×26×1	14×26×1	14×26×1	14×26×1
Fluid Cell Size	3.6mm× 4.8mm× 10mm	1.8mm× 2.4mm× 5mm	0.9mm× 1.2mm× 2.5mm	0.45mm× 0.6mm× 1.25mm
Total Number of DEM Cells	44×95×20	44×95×20	44×95×20	44×95×20
Nominal Pressure	1 bar	1 bar	1 bar	1 bar
Temperature	298.15K	298.15K	298.15K	298.15K
Fluid Density	1.13 kg/m^2	1.13 kg/m^2	1.13 kg/m^2	1.13 kg/m^2
Time Step Size	2.6×10^{-6} sec	1.3×10^{-6} sec	6.5×10^{-7} sec	3.25×10^{-7} sec
Number of Particles	9240	9240	9240	9240
Size of Particles	1.2± 0.05mm	0.6± 0.025mm	0.3± 0.0125mm	0.15± 0.00625mm
Particle Density	1000 kg/m^2	1000 kg/m^2	1000 kg/m^2	1000 kg/m^2
Young Modulus of Particles	1.2×10^8 Pa	1.2×10^8 Pa	1.2×10^8 Pa	1.2×10^8 Pa
Poisson Ratio	0.3	0.3	0.3	0.3
Coefficient of Normal Restitution	0.986	0.986	0.986	0.986
Coefficient of Friction	0.1	0.1	0.1	0.1

6. RESULTS

In the simulations, the particles are initialised in a regular pattern; therefore the positions of the particles must be randomised to create a mixed state (close to natural distribution of particles). Consequently, the bed was fluidised initially by applying high acceleration to fluid superficial velocity. Then superficial velocity was decreased in steps, and the pressure drop recorded at each superficial velocity. Bubbles caused the pressure drop to fluctuate, so the pressure drop signal was averaged over time. To check whether the results of the simulation were dependent on the time step, the simulation was run using time steps of 2.6×10^{-6} s, 1.95×10^{-6} s, 1.3×10^{-6} s and 6.5×10^{-7} s where same results were observed.

When the bed is fluidised the pressure drop (ΔP) across the bed is constant, and will only fall when the superficial velocity is below U_{MF}. CFD-DEM results for the averaged pressure drop, ΔP as a function of the superficial gas velocity for each size of particle are shown in

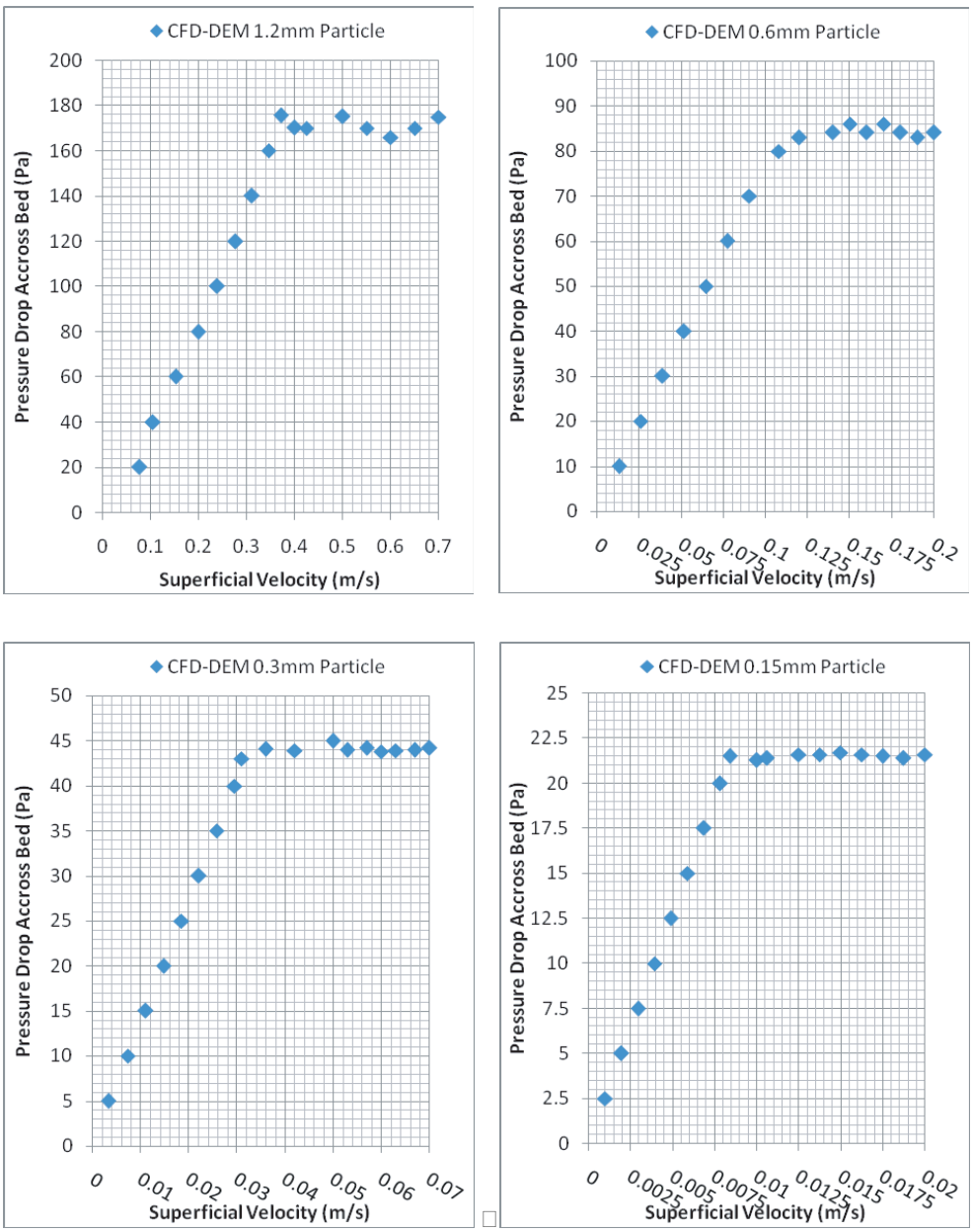

Figure 5 CFD-DEM simulation results.

Figure 5. The value of U_{MF} was obtained by the intersection of linear increasing pressure line and constant pressure line) in each case. The U_{MF} as a function of the particle diameter is shown in Figure 6, along with the theoretical values from Ergun's equation (Eqn. (5), using the average voidage from the simulation), and the correlations of Wen and Yu (1966) and Chitester et al. (1984).

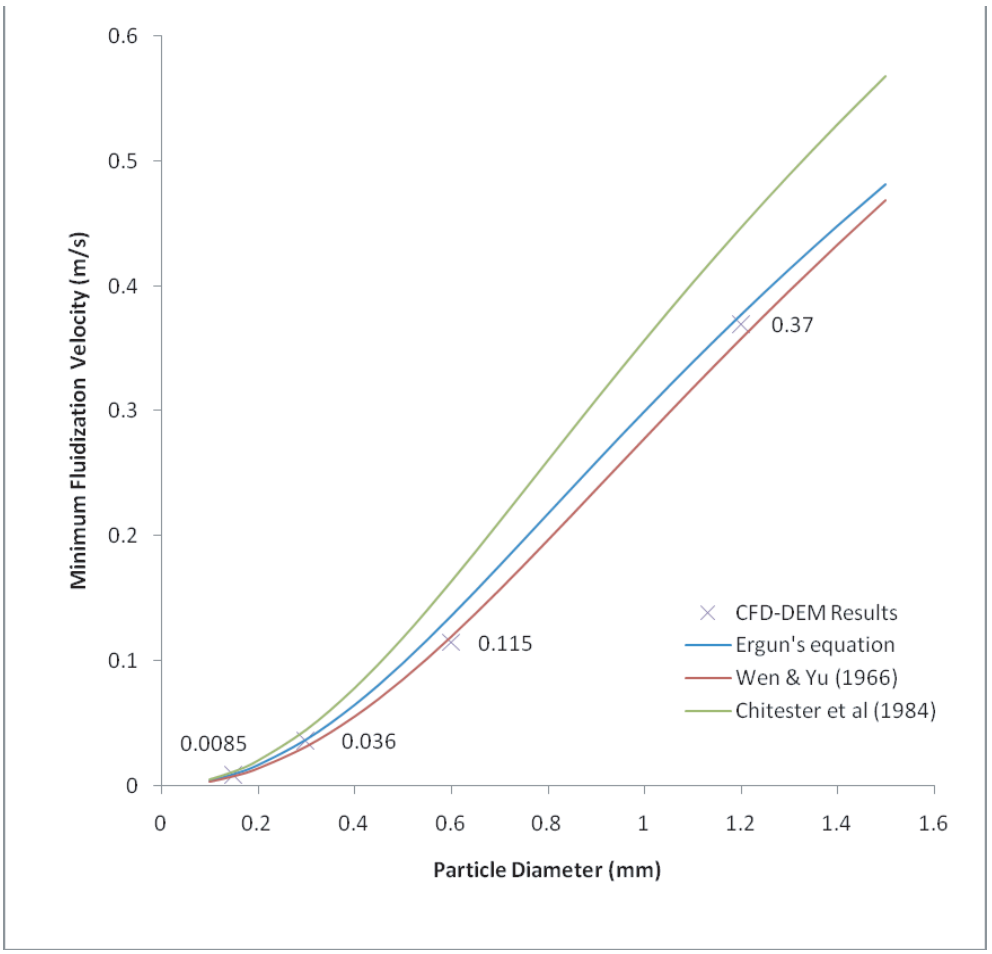

Figure 6 U_{MF} versus particle diameters

7. CONCLUSION

Minimum fluidisation velocities for fluidised bed were computed via CFD-DEM simulations. For the same conditions minimum fluidisation velocity were calculated using the correlations given in literature. The results were compared as given in Figure 6. It has been found that results are in close agreement.

REFERENCES

[1] Anderson J.D. (1995). Computational fluid dynamics, McGraw-Hill, 237–239.

[2] Anderson T.B, Jackson R. (1967). Industrial and Engineering Chemistry Fundamentals, 6, 4, 527–539.

[3] Beetstra R., Van der Hoef, M.A., Kuipers J.A.M. (2007). Numerical study of segregation using a new drag force correlation for polydisperse systems derived from Lattice Boltzmann simulations. Chemical Engineering Science, 62,246–255.

[4] Chitester D. C., Kornosky M. R., Fan L. S. and Danko J. P. (1984) Characteristics of fluidization at high pressure, Chemical Engineering Science, 39, 253–261.

[5] Courant R, Friedrichs K, Lewy H. (1967) On the partial difference equations of mathematical physics, IBM Journal, 215–234.

[6] Cundall P, & Strack O. (1979) A discrete element model for granular assemblies, Geotechnique, 29, 47.

[7] Hairer, Nørsett, Wanner, Gerhard (1993) Solving ordinary differential equations I: Nonstiff problems, Springer Verlag.

[8] Hertz H. (1882) Uber die Beruhrang fester elastischer Korper (On the contact of elastic solids), Journal der rennin und angewandeten Mathematik. 92, S. 156–171.

[9] Kunii D. and Levenspiel O. (1991). Fluidization Engineering. Butterworth-Heinemann, Stoneham, USA

[10] Lee S. and Lee L. (2005) Encyclopaedia of Chemical Processing, CRC Press, Boca Raton, Florida

[11] Mindlin R. D. & Deresiewicz H. (1953) Elastic Spheres in Contact under Varying Oblique Forces, Journal of Applied Mechanics, 20, 327.

[12] Tsuji Y, Kawaguchi T, & Tanaka T. (1992) Discrete particle simulation of two-dimensional fluidised bed, Powder Technology, 77, 79–87.

[13] Wen C. Y. and Yu Y. H. (1966) A generalized method for predicting the minimum fluidization velocity, AIChE Journal, 12, 610–612.